

Effect of slip and heat transfer on peristaltic transport of a Jeffrey fluid in a vertical asymmetric porous channel

P. Lakshminarayana^{1*}, S. Sreenadh², G. Sucharitha¹ and K. Nandagopal¹

¹*Department of Mathematics, Sree Vidya Nikethan Engineering College, Tirupati, India*

²*Department of Mathematics, Sri Venkateswara University, Tirupati, India*

ABSTRACT

This paper deals with the influence of slip and heat transfer on the peristaltic transport of a Jeffrey fluid in a vertical asymmetric channel with porous medium. The governing equations are solved by using perturbation technique. The expressions for the temperature, the axial velocity and pressure gradient are obtained. The impact of various physical parameters on the velocity, the temperature and the pressure rise are discussed through graphs. It is believed that the results presented here will find prospective application in the study of various fluid mechanical problems associated with gastrointestinal tract, intra pleural membranes, capillary walls and small blood vessels.

Keywords: Peristaltic transport, Heat transfer, Jeffrey fluid, Porous medium, Slip, vertical asymmetric channel.

INTRODUCTION

Peristalsis is a well known mechanism for mixing and transporting fluid which is generated by a progressive wave of contraction or expansion moving on the wall of the tube. It occurs widely in many biological and biomedical systems. It is an inherent property of many tubular organs of the human body. It plays an indispensable role in transporting many physiological fluids in the body in various situations such as swallowing food through the esophagus, movement of chyme in the gastro-intestinal tract, urine transport from the kidneys to the urinary bladder through the ureter, the transport of spermatozoa in the ductus efferentes of the male reproductive tract and in the cervical canal, movement of lymphatic fluids in lymphatic vessels and circulation of blood in small blood vessels. Also peristalsis involves in many industrial and biomedical applications.

Peristaltic transport has been studied under various conditions by using different assumptions like long wavelength or small amplitude ratio. Shapiro et al. [1] studied peristaltic pumping with long wavelength at low Reynolds number. Manton [2] considered an asymptotic expansion for flow in an axisymmetric pipe with long peristaltic waves of arbitrary shape. Fung and Yih [3], Jaffrin and Shapiro [4] many aspects were made to study peristaltic flow of different types of fluids under different conditions. Radhakrishnamacharya [5] has investigated long wavelength approximation to peristaltic motion of a power law fluid. Shukla and Gupta [6] studied the peristaltic transport of a power law fluid with variable consistency, Srivastava and Srivastava [7] discussed the peristaltic transport of blood: Casson model II. Takabatake and Ayukawa [8] studied the two-dimensional peristaltic flows numerically. Weinberg et al. [9] made an experimental study of peristaltic pumping. Yin and Fung [10] investigated the comparison of theory and experiment in peristaltic transport. Srivastava and Saxena [11] studied a two-fluid model of non-Newtonian blood flow induced by peristaltic waves. Peristaltic flow of micropolar fluid in an asymmetric channel with permeable walls is discussed by Sreenadh et al. [12]. Sucharitha et al. [13, 14] described the peristaltic flow of non-Newtonian fluids in an asymmetric channel with porous medium.

The interaction of peristalsis with heat transfer has not received much attention. The thermodynamical aspects of blood may not be important when blood is inside the body but they become significant when it is drawn out of the body. Keeping in view the significance of heat transfer in blood flow, Srinivas and Kothandapani [15] analyzed the

influence of heat and mass transfer on MHD peristaltic flow through a porous space with compliant walls. Lakshminarayana et al. [16] have reported the influence of heat transfer on MHD peristaltic flow through a vertical asymmetric porous channel. Vajravelu et al. [17] studied the influence of heat transfer on peristaltic transport of a Jeffrey fluid in a vertical porous stratum. Agrawal [18] discussed the heat transfer to pulsatile flow of a conducting fluid through a porous channel in the presence of magnetic field. Tang et al. [19] investigated the peristaltic flow of a heat conducting fluid subject to a prescribed pressure drop. Radhakrishnamacharya and Srinivasulu [20] studied the influence of wall properties on peristaltic transport with heat transfer.

All the above investigations on peristaltic transport have been done taking into account the classical no slip boundary condition. However, in several applications, the flow pattern corresponds to a slip flow and the fluid presents a loss of adhesion at the wetted wall making the fluid slide along the wall. Beavers and Joseph [21] investigate the fluid flow at the interface between a porous medium and fluid layer in an experimental study and proposed a slip boundary condition at the interface. Flows with slip would be useful for problems in chemical engineering, for example flows through pipes in which chemical reactions occur at the walls, two-phase flows in porous slider bearings. Saffman [22] proposed an improved slip boundary condition.

Physiological researches (de Vries et al. [23]) indicate that uterine peristalsis resulting from myometrial contraction can take place in both symmetric and asymmetric directions. In different studies pertaining to the gastrointestinal tract, intra-pleural membranes, capillary walls, human lung, bile duct, gall bladder with stones and small blood vessels, flow in porous tubes and deformable porous layers have been examined by different authors. As mentioned by Keener and Sneyd [24], gastrointestinal tract is surrounded by a number of heavily innervated muscle layers which are smooth muscles consisting of many folds. Bergel [25] observed that the capillary walls are surrounded by flattened endothelial cell layers which are permeable. Ramana Kumari and Radhakrishnamacharya [26] studied the effect of slip on heat transfer to peristaltic transport in the presence of magnetic field with wall effects. Arun Kumar et al. [27] examined the influence of partial slip on the peristaltic transport of a micropolar fluid in an inclined asymmetric channel. Hayat et al. [28] investigated the influence of partial slip on the peristaltic flow in a porous channel. Vajravelu et al. [30] analyzed the peristaltic transport of a conducting Jeffrey fluid in an inclined asymmetric channel. Sreenadh et al. [31] studied the effect of MHD on peristaltic transport of a Pseudoplastic fluid in an asymmetric channel With porous medium. Lakshminarayana et al. [32] examined the peristaltic pumping of a conducting fluid in a channel with a porous peripheral layer.

In view of all the aforesaid observations and remarks, in this paper, the interaction of non-linear peristaltic transport with heat transfer for a Jeffrey fluid with slip boundary condition in a vertical asymmetric porous channel is studied. A perturbation method of solution has been obtained in terms of various parameters and analytical solutions have been obtained for velocity and temperature. The expression for pressure rise is obtained. The effects of different pertinent parameters on average velocity, heat transfer coefficient and pressure rise have been studied.

2. Mathematical formulation

Consider the motion of a Jeffrey fluid in two dimensional vertical asymmetric porous channel. The sinusoidal waves propagated along the channel walls are of the following forms

$$\begin{aligned}\bar{Y} = H_1 &= d_1 + a_1 \cos \left[\frac{2\pi}{\lambda} (\bar{X} - c\bar{t}) \right] \quad (\text{upper wall}) \\ \bar{Y} = H_2 &= -d_2 - b_1 \cos \left[\frac{2\pi}{\lambda} (\bar{X} - c\bar{t}) + \phi \right] \quad (\text{lower wall})\end{aligned} \quad (1)$$

where λ is the wave length, $d_1 + d_2$ is the width of the channel, a_1 and b_1 are the amplitudes of the waves, the phase difference ϕ varies in the range $0 \leq \phi \leq \pi$, $\phi = 0$ corresponds to symmetric channel with waves are out of phase and $\phi = \pi$ with waves are in phase, and further a_1, b_1, d_1, d_2 and ϕ satisfy the condition [29]

$$a_1^2 + b_1^2 + 2a_1b_1 \cos \phi \leq (d_1 + d_2)^2 \quad (2)$$

The governing equations are

$$\frac{\partial \bar{U}}{\partial \bar{X}} + \frac{\partial \bar{V}}{\partial \bar{Y}} = 0 \quad (3)$$

Momentum equations

$$\rho_0 \left(\frac{\partial \bar{U}}{\partial t} + \bar{U} \frac{\partial \bar{U}}{\partial \bar{X}} + \bar{V} \frac{\partial \bar{U}}{\partial \bar{Y}} \right) = -\frac{\partial \bar{P}}{\partial \bar{X}} + \frac{\partial S_{\bar{X}\bar{X}}}{\partial \bar{X}} + \frac{\partial S_{\bar{X}\bar{Y}}}{\partial \bar{Y}} - \frac{\mu}{k} \bar{U} + \rho_0 g \beta (T - T_0) \quad (4)$$

$$\rho_0 \left(\frac{\partial \bar{V}}{\partial t} + \bar{U} \frac{\partial \bar{V}}{\partial \bar{X}} + \bar{V} \frac{\partial \bar{V}}{\partial \bar{Y}} \right) = -\frac{\partial \bar{P}}{\partial \bar{Y}} + \frac{\partial S_{\bar{X}\bar{Y}}}{\partial \bar{X}} + \frac{\partial S_{\bar{Y}\bar{Y}}}{\partial \bar{Y}} - \frac{\mu}{k} \bar{V} \quad (5)$$

Energy equation

$$\rho_0 c_p \left(\frac{\partial T}{\partial t} + \bar{U} \frac{\partial T}{\partial \bar{X}} + \bar{V} \frac{\partial T}{\partial \bar{Y}} \right) = K_0 \left(\frac{\partial^2 T}{\partial \bar{X}^2} + \frac{\partial^2 T}{\partial \bar{Y}^2} \right) + 2\mu \left(\left(\frac{\partial \bar{U}}{\partial \bar{X}} \right)^2 + \left(\frac{\partial \bar{V}}{\partial \bar{Y}} \right)^2 \right) + \mu \left(\frac{\partial \bar{V}}{\partial \bar{X}} + \frac{\partial \bar{U}}{\partial \bar{Y}} \right)^2 + \frac{\mu}{k} \bar{U}^2 \quad (6)$$

here \bar{U}, \bar{V} are velocity components in the laboratory frame, ρ_0 is density, μ is coefficient of viscosity of the fluid, g is the acceleration due to gravity, T is the temperature of the fluid, T_0 is the mean value of T_1 and T_2 , P is the pressure β is the coefficient of thermal expansion. c_p is the specific heat at constant pressure, k_0 is the thermal conductivity, k is the permeability parameter.

The transformation between wave frame (\bar{x}, \bar{y}) moving with velocity c and the fixed frame (\bar{X}, \bar{Y}) is given by

$$\bar{x} = \bar{X} - c\bar{t}, \quad \bar{y} = \bar{Y}, \quad \bar{u} = \bar{U} - c, \quad \bar{v} = \bar{V}, \quad \bar{p}(\bar{x}) = \bar{P}(\bar{X}, \bar{t}) \quad (7)$$

where $\bar{U}, \bar{V}, \bar{P}$ are the velocity components, pressure in the laboratory frame and $\bar{u}, \bar{v}, \bar{p}$ are the velocity components, pressure in the wave frame respectively.

We introduce the following non-dimensional quantities:

$$\left. \begin{aligned} x &= \frac{\bar{x}}{\lambda}, \quad y = \frac{\bar{y}}{d_1}, \quad u = \frac{\bar{u}}{c}, \quad v = \frac{\bar{v}}{c\delta}, \quad \delta = \frac{d_1}{\lambda}, \quad p = \frac{d_1^2 \bar{p}}{\mu c \lambda}, \quad t = \frac{c\bar{t}}{\lambda}, \quad h_1 = \frac{H_1}{d_1}, \\ h_2 &= \frac{H_2}{d_1}, \quad \text{Re} = \frac{\rho_0 c d_1}{\mu}, \quad d = \frac{d_2}{d_1}, \quad a = \frac{a_1}{d_1}, \quad b = \frac{b_1}{d_1}, \quad M^2 = \frac{\sigma B_0^2 d_1^2}{\mu}, \quad \sigma = \frac{d_1}{\sqrt{k}} \\ T &= \theta(T_1 - T_0) + T_0, \quad h = \frac{(T_2 - T_0)}{(T_1 - T_0)}, \quad \text{Pr} = \frac{\mu c_p}{k_0}, \quad S = \frac{d_1 \bar{S}}{\mu c}, \quad \text{Ec} = \frac{c^2}{c_p (T_1 - T_0)}, \\ N &= \text{Ec Pr}, \quad \text{Gr} = \frac{\beta g (T_1 - T_0) d_1^2}{\nu c} \end{aligned} \right\} \quad (8)$$

where Re is the Reynolds number, δ is the dimensionless wave number, σ is the permeability parameter, Gr is the Grashof number, Pr is the Prandtl number, ν is the kinematic viscosity, Ec is the Eckert number, and N is the perturbation parameter.

The equations governing the flow become

$$\frac{\partial u}{\partial x} + \frac{\partial v}{\partial y} = 0 \tag{9}$$

$$\delta R \left[(u+1) \frac{\partial u}{\partial x} + v \frac{\partial u}{\partial y} \right] = -\frac{\partial p}{\partial x} + \frac{\partial S_{xx}}{\partial x} \delta + \frac{\partial S_{xy}}{\partial y} - \sigma^2 (u+1) + Gr \theta \tag{10}$$

$$\delta^3 R \left[(u+1) \frac{\partial v}{\partial x} + v \frac{\partial v}{\partial y} \right] = -\frac{\partial p}{\partial x} + \frac{\partial S_{xy}}{\partial x} \delta^2 + \frac{\partial S_{yy}}{\partial y} \delta - \delta^2 \sigma^2 v \tag{11}$$

$$\delta Pr R \left[(u+1) \frac{\partial \theta}{\partial x} + v \frac{\partial \theta}{\partial y} \right] = \left[\frac{\partial^2 \theta}{\partial x^2} \delta^2 + \frac{\partial^2 \theta}{\partial y^2} \right] + 2\delta^2 N \left[\left(\frac{\partial u}{\partial x} \right)^2 + \left(\frac{\partial v}{\partial y} \right)^2 \right] + N \left(\delta^2 \frac{\partial v}{\partial x} + \frac{\partial u}{\partial y} \right)^2 + N \sigma^2 (u+1)^2 \tag{12}$$

where $S_{xx} = \frac{2\delta}{1+\lambda_1} \left[1 + \frac{\delta \lambda_2 c}{a} \left(u \frac{\partial}{\partial x} + \frac{v}{\delta} \frac{\partial}{\partial y} \right) \right] \frac{\partial u}{\partial x}$,

$$S_{xy} = \frac{1}{1+\lambda_1} \left[1 + \frac{\delta \lambda_2 c}{a} \left(u \frac{\partial}{\partial x} + \frac{v}{\delta} \frac{\partial}{\partial y} \right) \right] \left(\frac{\partial u}{\partial y} + \delta \frac{\partial v}{\partial x} \right),$$

$$S_{yy} = \frac{-2\delta}{1+\lambda_1} \left[1 + \frac{\delta \lambda_2 c}{a} \left(u \frac{\partial}{\partial x} + \frac{v}{\delta} \frac{\partial}{\partial y} \right) \right] \frac{\partial u}{\partial y}, \quad \text{and} \quad \left(\frac{\partial s_{xy}}{\partial y} \right)_{\delta \rightarrow 0} = \frac{1}{1+\lambda_1} \frac{\partial^2 u}{\partial y^2}.$$

The non-dimensional boundary conditions are

$$u + L \frac{\partial u}{\partial y} = -1 \quad \text{and} \quad \theta = 1 \quad \text{at} \quad y = h_1(x)$$

$$u - L \frac{\partial u}{\partial y} = -1 \quad \text{and} \quad \theta = n \quad \text{at} \quad y = h_2(x) \tag{13}$$

where L is the non dimensional slip parameter. Using the long wave length approximation and dropping terms of order δ and higher, equations governing equations are reduced to

$$0 = -\frac{\partial p}{\partial x} + \frac{1}{1+\lambda_1} \frac{\partial^2 u}{\partial y^2} - \sigma^2 (u+1) + Gr \theta \tag{14}$$

$$0 = -\frac{\partial p}{\partial y} \tag{15}$$

$$0 = \frac{\partial^2 \theta}{\partial y^2} + N \left(\frac{\partial u}{\partial y} \right)^2 + N \sigma^2 (u+1)^2 \tag{16}$$

3. Solution of the problem

Equations (14) and (16) are coupled and non-linear. Hence they are difficult to solve. However the fact N is small in most practical problems allows us to employ a perturbation technique to solve these non-linear equations. We write

$$(u, \theta, p) = (u_0, \theta_0, p_0) + N (u_1, \theta_1, p_1) + \dots \tag{17}$$

Using the above relation in equations (13), (14) and (16) we obtain a system of equations of different orders.

3.1. System of order N^0

The governing equations of the zeroth order are

$$0 = -\frac{dp_0}{dx} + \frac{1}{1+\lambda_1} \frac{\partial^2 u_0}{\partial y^2} - \sigma^2(u_0 + 1) + Gr \theta_0 \tag{18}$$

$$0 = \frac{\partial^2 \theta_0}{\partial y^2}. \tag{19}$$

The appropriate boundary conditions are

$$\left. \begin{aligned} u_0 + L \frac{\partial u_0}{\partial y} = -1 \quad \text{and} \quad \theta_0 = 1 \quad \text{at} \quad y = h_1(x) \\ u_0 - L \frac{\partial u_0}{\partial y} = -1 \quad \text{and} \quad \theta_0 = n \quad \text{at} \quad y = h_2(x). \end{aligned} \right\} \tag{20}$$

solving the equations (18) and (19) with the use of boundary conditions (20) and we obtain the zeroth-order velocity and the temperature as

$$u_0 = c_3 \cosh \sigma \sqrt{1+\lambda_1} y + c_4 \sinh \sigma \sqrt{1+\lambda_1} y - \frac{1}{\sigma^2} \left[\frac{dp_0}{dx} + \sigma^2 - Gr(c_1 y + c_2) \right] \tag{21}$$

$$\theta_0 = c_1 y + c_2 \tag{22}$$

where

$$c_1 = \frac{1-n}{h_1-h_2}, \quad c_2 = \frac{nh_1-h_2}{h_1-h_2}, \quad c_3 = \frac{1}{\sigma^2} \frac{dp_0}{dx} s_9 + s_{10}, \quad c_4 = s_7 \left(1 - \frac{1}{\sigma^2} \frac{dp_0}{dx} \right) - s_8$$

Using the relation (17) we obtain zeroth-order dimensionless mean flow in the laboratory and in the wave frames as

$$\Theta_0 = F_0 + 1, \quad F_0 = \int_0^h u_0 dy,$$

Where

$$F_0 = \frac{dp_0}{dx} \left(\frac{s_{11} - s_{12} - h_1 + h_2}{\sigma^2} \right) + s_{13} + s_{14} - s_{15} + s_{16} \tag{23}$$

The corresponding pressure gradient is given by

$$\frac{dp_0}{dx} = \frac{\sigma^2 (F_0 - s_{13} - s_{14} + s_{15} - s_{16})}{s_{11} - s_{12} - h_1 + h_2} \tag{24}$$

Also, the non-dimensional zeroth-order pressure rise is given by

$$\Delta p_0 = \int_0^1 \frac{dp_0}{dx} dx. \tag{25}$$

3.2. System of order N^1

The governing equations and the appropriate boundary conditions for the first order are

$$0 = -\frac{dp_1}{dx} + \frac{1}{1+\lambda_1} \frac{\partial^2 u_1}{\partial y^2} - \sigma^2 u_1 + Gr \theta_1, \tag{26}$$

$$0 = \frac{\partial^2 \theta_1}{\partial y^2} + \left(\frac{\partial u_0}{\partial y} \right)^2 + \sigma^2 (u_0 + 1)^2, \tag{27}$$

$$\left. \begin{aligned} u_1 + L \frac{\partial u_1}{\partial y} &= -1 \quad \text{and} \quad \theta_1 = 1 \quad \text{at} \quad y = h_1(x) \\ u_1 - L \frac{\partial u_1}{\partial y} &= -1 \quad \text{and} \quad \theta_1 = n \quad \text{at} \quad y = h_2(x) \end{aligned} \right\} \tag{28}$$

Solving the equations (26) and (27) with the use of boundary conditions (28) we obtain

$$u_1 = c_7 \cosh \sigma \sqrt{1 + \lambda_1} y + c_8 \sinh \sigma \sqrt{1 + \lambda_1} y - \frac{1}{\sigma^2} \frac{dp_1}{dx} - Gr \left\{ \begin{aligned} &\frac{1}{3\sigma^2} (s_{25} \cosh 2\sigma \sqrt{1 + \lambda_1} y - s_{26} \sinh 2\sigma \sqrt{1 + \lambda_1} y) + \cosh \sigma \sqrt{1 + \lambda_1} y (s_{53} y^2 + s_{54} y - s_{55}) \\ &+ \sinh \sigma \sqrt{1 + \lambda_1} y (s_{56} y^2 + s_{57} y - s_{58}) + \frac{s_{17}}{4} y^4 + \frac{s_{32}}{3\sigma^2} y^3 - s_{50} y^2 - s_{51} y - s_{52} \end{aligned} \right\} \tag{29}$$

$$\theta_1 = s_{25} \cosh 2\sigma \sqrt{1 + \lambda_1} y - s_{26} \sinh 2\sigma \sqrt{1 + \lambda_1} y + s_{28} \sinh \sigma \sqrt{1 + \lambda_1} y + s_{29} \cosh \sigma \sqrt{1 + \lambda_1} y - s_{30} (c_1 y + c_2) [c_4 \sinh \sigma \sqrt{1 + \lambda_1} y + c_3 \cosh \sigma \sqrt{1 + \lambda_1} y] + \frac{s_{31}}{2} y^2 - \frac{s_{32}}{3} y^3 - \frac{\sigma^2 s_{17}^2}{12} y^4 + c_5 y + c_6 \tag{30}$$

where

$$c_5 = \frac{s_{39} + s_{40} + s_{41} - s_{42}}{h_2 - h_1}, \quad c_6 = s_{43} - s_{44} + s_{45} + s_{46} - c_5 h_1, \\ c_7 = \frac{1}{s_2} \left(\frac{1}{\sigma^2} \frac{dp_1}{dx} + Gr (s_{71} + L s_{72}) - c_8 s_2 \right), \quad c_8 = \frac{1}{s_2 s_4 - s_1 s_5} \left(\frac{1}{\sigma^2} \frac{dp_1}{dx} (s_4 - s_1) + Gr s_{83} \right)$$

Using the relation (19) we obtain first-order dimensionless mean flow in the laboratory and in the wave frames as

$$\Theta_1 = F_1, \quad F_1 = \int_0^h u_1 dy,$$

$$\text{in which } F_1 = \frac{dp_1}{dx} s_{97} + s_{100} \tag{31}$$

The corresponding pressure gradient is given by

$$\frac{dp_1}{dx} = \frac{(F_1 - s_{100})}{s_{97}} \tag{32}$$

The non-dimensional first-order pressure rise is given by

$$\Delta p_1 = \int_0^1 \frac{dp_1}{dx} dx. \tag{33}$$

The expression for the velocity is given by

$$u = u_0 + N u_1 \tag{37}$$

where u_0 and u_1 are given by the equations (21) and (29). The expression for the temperature field is

$$\theta = \theta_0 + N \theta_1 \quad (38)$$

where θ_0 and θ_1 are given by the equations (22) and (30).

The expression for the pressure rise is

$$\Delta p = \Delta p_0 + N \Delta p_1 \quad (39)$$

where Δp_0 and Δp_1 are given by the equations (25) and (33).

RESULTS AND DISCUSSION

Equation (37) gives the expression for velocity in terms of y . Velocity profiles are plotted in *Fig.1* to study the effects of the physical parameters (such as the permeability parameter σ , the slip parameter L , the Grashof number Gr , the phase difference ϕ , the Jeffrey parameter λ_1 and the perturbation parameter N) on the velocity distribution in the vertical asymmetric porous channel. *Fig.1a* is drawn to study the effect of λ_1 on the velocity. It reveals that the velocity profiles are parabolic. We observe that the velocity decreases with increasing λ_1 and intersect near the centre of the channel further opposite behaviour is observed. *Fig.1b* is plotted to study the effect of σ on the velocity. We observe that the velocity decreases with increasing σ . From *Fig.1c*, we see that the velocity decreases with an increase in L . *Fig.1d*, *Fig.1e* and *Fig.1f* are plotted for velocity for different values of N , Gr and ϕ . We notice that velocity increases with the increase in N , Gr and decrease in ϕ .

Temperature field is calculated from equation (38) in terms of y . Temperature profiles are plotted in *Fig.2* to study the effects of the physical parameters of the problem. *Fig.2a* is drawn to study the effect of λ_1 on the temperature distribution in the vertical asymmetric porous channel. It is observed that the temperature increases with increasing λ_1 and the temperature profiles are parabolic throughout the channel. *Fig.2b* is drawn to study the effect of σ on the temperature. It is notice that the temperature increases with increasing σ . From *Fig.2c* we find that the temperature increases with an increase in L . *Fig.2d*, *Fig.2e* and *Fig.2f* are plotted for different values of N , Gr and ϕ . We notice that the increase in N , Gr increases the temperature. Also observe that the increase in ϕ decreases the temperature.

Equation (39) gives the expression for the pressure rise ΔP in terms of the mean flow Θ . The variation of pressure rise with the mean flow for different values of λ_1 is shown in *Fig.3a*. We observe that for a given Θ , ΔP increases with increasing λ_1 . *Fig.3b* shows the variation of pressure rise with the mean flow for different values of σ . We notice that pressure rise increases when σ increases. The variation of pressure rise with the mean flow for different values of L is shown in *Fig.3c*. We find that ΔP decreases with increasing L . *Fig.3d* depicts that pressure rise decreases when N increases. From *Fig.3e* we observe that ΔP increases with increasing Gr . *Fig.3f* describes that pressure rise decreases when ϕ increases.

Appendix

$$s_1 = \cosh \sigma \sqrt{1+\lambda_1} h_1 + (L \sigma \sqrt{1+\lambda_1}) \sinh \sigma \sqrt{1+\lambda_1} h_1, \quad s_2 = \sinh \sigma \sqrt{1+\lambda_1} h_1 + (L \sigma \sqrt{1+\lambda_1}) \cosh \sigma \sqrt{1+\lambda_1} h_1$$

$$s_3 = \frac{Gr(c_1(L+h_1)+c_2) - \sigma^2}{\sigma^2}, \quad s_4 = \cosh \sigma \sqrt{1+\lambda_1} h_2 - (L \sigma \sqrt{1+\lambda_1}) \sinh \sigma \sqrt{1+\lambda_1} h_2$$

$$s_5 = \sinh \sigma \sqrt{1+\lambda_1} h_2 - (L \sigma \sqrt{1+\lambda_1}) \cosh \sigma \sqrt{1+\lambda_1} h_2, s_6 = \frac{Gr(c_1(h_2-L)+c_2)-\sigma^2}{\sigma^2}$$

$$s_7 = \frac{s_1-s_4}{s_2s_4-s_1s_5}, s_8 = \frac{s_3s_4-s_1s_6}{s_2s_4-s_1s_5}, s_9 = \frac{1+s_2s_7}{s_1}, s_{10} = \frac{s_2s_8-s_2s_7-s_3-1}{s_1}$$

$$s_{11} = \frac{s_9(\sinh \sigma \sqrt{1+\lambda_1} h_1 - \sinh \sigma \sqrt{1+\lambda_1} h_2)}{\sigma \sqrt{1+\lambda_1}}, s_{12} = \frac{s_7(\cosh \sigma \sqrt{1+\lambda_1} h_1 - \cosh \sigma \sqrt{1+\lambda_1} h_2)}{\sigma \sqrt{1+\lambda_1}}$$

$$s_{13} = \frac{s_{10}(\sinh \sigma \sqrt{1+\lambda_1} h_1 - \sinh \sigma \sqrt{1+\lambda_1} h_2)}{\sigma \sqrt{1+\lambda_1}}, s_{14} = \frac{(s_7-s_8)(\cosh \sigma \sqrt{1+\lambda_1} h_1 - \cosh \sigma \sqrt{1+\lambda_1} h_2)}{\sigma \sqrt{1+\lambda_1}}$$

$$s_{15} = \frac{(h_1-h_2)(\sigma^2-Gr c_2)}{\sigma^2}, s_{16} = \frac{(h_1^2-h_2^2)Gr c_1}{2\sigma^2}, s_{17} = \frac{Gr c_1}{\sigma^2}, s_{18} = -\frac{dp_0/dx}{\sigma^2},$$

$$s_{19} = \frac{\sigma^2(c_3^2(1+\lambda_1)+c_4^2)}{2}, s_{20} = \frac{\sigma^2(c_4^2(1+\lambda_1)+c_3^2)}{2}, s_{21} = \sigma^2 c_3 c_4 (2+\lambda_1), s_{22} = 2\sigma(\sqrt{1+\lambda_1}s_{17}c_3 + \sigma c_4 s_{18}),$$

$$s_{23} = 2\sigma(\sqrt{1+\lambda_1}s_{17}c_4 + \sigma c_3 s_{18}), s_{24} = s_{17}^2 + \sigma^2 s_{18}^2, s_{25} = \frac{-s_{19}-s_{20}}{(2\sigma\sqrt{1+\lambda_1})^2}, s_{26} = \frac{s_{21}}{(2\sigma\sqrt{1+\lambda_1})^2},$$

$$s_{27} = \frac{2Gr c_1}{(2\sigma\sqrt{1+\lambda_1})^2} \left(1 + \frac{1}{\sigma\sqrt{1+\lambda_1}}\right), s_{28} = s_{27}c_3 - \frac{s_{22}}{(\sigma\sqrt{1+\lambda_1})^2}, s_{29} = s_{27}c_4 - \frac{s_{23}}{(\sigma\sqrt{1+\lambda_1})^2}$$

$$s_{30} = \frac{2Gr}{(\sigma\sqrt{1+\lambda_1})^2}, s_{31} = s_{19} - s_{20} - s_{24} - 2s_{18}Gr c_2 - \frac{Gr^2 c_2^2}{\sigma^2}, s_{32} = s_{18}Gr c_1 + \frac{Gr^2 c_1 c_2}{\sigma^2},$$

$$s_{33} = \cosh 2\sigma\sqrt{1+\lambda_1} h_1 - \cosh 2\sigma\sqrt{1+\lambda_1} h_2, s_{34} = \sinh 2\sigma\sqrt{1+\lambda_1} h_1 - \sinh 2\sigma\sqrt{1+\lambda_1} h_2$$

$$s_{35} = \sinh \sigma\sqrt{1+\lambda_1} h_1 - \sinh \sigma\sqrt{1+\lambda_1} h_2, s_{36} = \cosh \sigma\sqrt{1+\lambda_1} h_1 - \cosh \sigma\sqrt{1+\lambda_1} h_2$$

$$s_{37} = (c_1h_1+c_2)(c_4 \sinh \sigma\sqrt{1+\lambda_1} h_1 + c_3 \cosh \sigma\sqrt{1+\lambda_1} h_1),$$

$$s_{38} = (c_1h_1+c_2)(c_4 \sinh \sigma\sqrt{1+\lambda_1} h_2 + c_3 \cosh \sigma\sqrt{1+\lambda_1} h_2), s_{39} = s_{25} s_{33} - s_{26} s_{34} + s_{28} s_{35},$$

$$s_{40} = s_{29} s_{36} - s_{30}(s_{37} - s_{38}), s_{41} = \left(\frac{h_1^2-h_2^2}{2}\right) \left(s_{31} - \sigma^2 s_{17}^2 \left(\frac{h_1^2+h_2^2}{6}\right)\right), s_{42} = s_{32} \left(\frac{h_1^3-h_2^3}{3}\right),$$

$$s_{43} = s_{26} \sinh 2\sigma\sqrt{1+\lambda_1} h_1 - s_{25} \cosh 2\sigma\sqrt{1+\lambda_1} h_1, s_{44} = s_{28} \sinh \sigma\sqrt{1+\lambda_1} h_1 + s_{29} \cosh \sigma\sqrt{1+\lambda_1} h_1$$

$$s_{45} = s_{30}(c_1h_1+c_2)(c_4 \sinh \sigma\sqrt{1+\lambda_1} h_1 + c_3 \cosh \sigma\sqrt{1+\lambda_1} h_1), s_{46} = s_{32} \frac{h_1^3}{3} + \sigma^2 s_{17}^2 \frac{h_1^4}{12} - s_{31} \frac{h_1^2}{2},$$

$$s_{47} = c_1c_4 \sinh \sigma\sqrt{1+\lambda_1}, s_{48} = 2c_4c_2\sigma\sqrt{1+\lambda_1} - c_3c_1, s_{49} = c_1c_3\sigma\sqrt{1+\lambda_1}, s_{50} = 2c_2c_3\sigma\sqrt{1+\lambda_1} - c_1c_4,$$

$$s_{51} = \frac{s_{31}(1+\lambda_1)-s_{17}^2}{2\sigma^2}, s_{52} = \frac{c_5\sigma^2(1+\lambda_1)-2s_{32}}{\sigma^4(1+\lambda_1)}, s_{53} = \frac{c_6\sigma^2(1+\lambda_1)^2-s_{31}(1+\lambda_1)-2s_{17}^2}{\sigma^4(1+\lambda_1)^2}$$

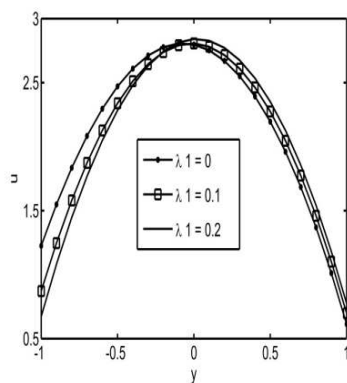
$$s_{54} = \frac{s_{30}s_{47}}{\sigma^2}, s_{55} = \frac{s_{30}s_{48}}{4\sigma^2} + \frac{\sqrt{1+\lambda_1}}{2\sigma}, s_{56} = \frac{s_{30}c_3c_2}{4\sigma^2}, s_{57} = \frac{s_{30}s_{49}}{4\sigma^2}, s_{58} = \frac{s_{30}s_{50}}{4\sigma^2} + \frac{s_{29}\sqrt{1+\lambda_1}}{2\sigma}, s_{59} = \frac{s_{30}c_4c_2}{4\sigma^2},$$

$$s_{60} = 2s_{54} + \sigma s_{58}\sqrt{1+\lambda_1}, s_{61} = s_{55} - \sigma\sqrt{1+\lambda_1} s_{59}, s_{62} = 2s_{57} + \sigma\sqrt{1+\lambda_1} s_{55}, s_{63} = s_{58} - \sigma\sqrt{1+\lambda_1} s_{56}$$

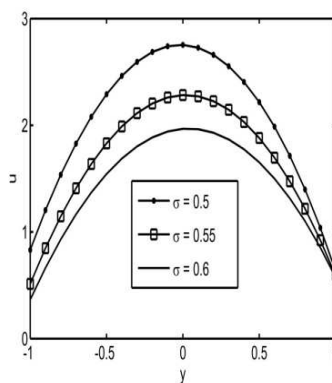
$$s_{64} = \cosh \sigma\sqrt{1+\lambda_1} h_1 (s_{54}h_1^2 + s_{55}h_1 - s_{56}), s_{65} = \sinh \sigma\sqrt{1+\lambda_1} h_1 (s_{57}h_1^2 + s_{58}h_1 - s_{59})$$

$$s_{66} = s_{17}^2 \frac{h_1^4}{12} + s_{32} \frac{h_1^3}{3\sigma^2} - s_{51}h_1^2 - s_{52}h_1 - s_{53}, s_{67} = s_{25} \sinh \sigma\sqrt{1+\lambda_1} h_1 - s_{26} \cosh \sigma\sqrt{1+\lambda_1} h_1$$

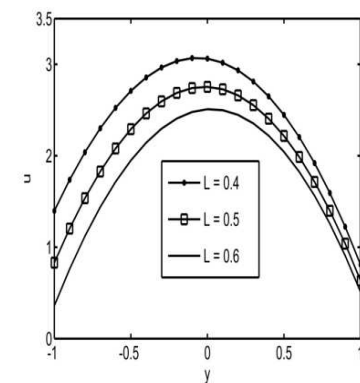
$$\begin{aligned}
 s_{68} &= \cosh \sigma \sqrt{1+\lambda_1} h_1 \left(\sigma \sqrt{1+\lambda_1} s_{57} h_1^2 + s_{60} h_1 + s_{61} \right), s_{69} = \sinh \sigma \sqrt{1+\lambda_1} h_1 \left(\sigma \sqrt{1+\lambda_1} s_{54} h_1^2 + s_{62} h_1 + s_{63} \right) \\
 s_{70} &= s_{17}^2 \frac{h_1^3}{3} + s_{32} \frac{h_1^2}{\sigma^2} - 2s_{51} h_1 - s_{52}, s_{71} = -s_{43} + s_{64} + s_{65} + s_{66}, s_{72} = \frac{\sqrt{1+\lambda_1} s_{67}}{3\sigma} + s_{68} + s_{69} + s_{70} \\
 s_{73} &= s_{25} \cosh 2\sigma \sqrt{1+\lambda_1} h_2 - s_{26} \sinh 2\sigma \sqrt{1+\lambda_1} h_2, s_{74} = \cosh \sigma \sqrt{1+\lambda_1} h_2 \left(s_{54} h_2^2 + s_{55} h_2 - s_{56} \right) \\
 s_{75} &= \sinh \sigma \sqrt{1+\lambda_1} h_2 \left(s_{57} h_2^2 + s_{58} h_2 - s_{59} \right), s_{76} = s_{17}^2 \frac{h_2^4}{12} + s_{32} \frac{h_2^3}{3\sigma^2} - s_{51} h_2^2 - s_{52} h_2 - s_{53} \\
 s_{77} &= s_{25} \sinh 2\sigma \sqrt{1+\lambda_1} h_2 - s_{26} \cosh 2\sigma \sqrt{1+\lambda_1} h_2, s_{78} = \cosh \sigma \sqrt{1+\lambda_1} h_2 \left(\sigma \sqrt{1+\lambda_1} s_{57} h_2^2 + s_{60} h_2 + s_{61} \right) \\
 s_{79} &= \sinh \sigma \sqrt{1+\lambda_1} h_2 \left(\sigma \sqrt{1+\lambda_1} s_{54} h_2^2 + s_{62} h_2 + s_{63} \right), s_{80} = s_{17}^2 \frac{h_2^3}{3} + s_{32} \frac{h_2^2}{\sigma^2} - 2s_{51} h_2 - s_{52} \\
 s_{81} &= \frac{s_{73}}{3\sigma^2} + s_{74} + s_{75} + s_{76}, s_{82} = \frac{\sqrt{1+\lambda_1} s_{77}}{3\sigma} + s_{78} + s_{79} + s_{80}, s_{83} = s_4 (s_{71} + L s_{72}) - s_1 (s_{81} - L s_{82}) \\
 s_{84} &= \frac{s_{25} s_{34} - s_{26} s_{33}}{6\sigma^3 \sqrt{1+\lambda_1}}, s_{85} = \frac{s_{35} (s_{54} (h_1^2 - h_2^2) + s_{55} (h_1 - h_2) - s_{56})}{\sigma \sqrt{1+\lambda_1}}, s_{86} = \frac{(2s_{54} (h_1 - h_2) + s_{55}) s_{36}}{(\sigma \sqrt{1+\lambda_1})^2}, \\
 s_{87} &= \frac{2s_{54} s_{35}}{(\sigma \sqrt{1+\lambda_1})^3}, s_{88} = \frac{s_{36} (s_{57} (h_1^2 - h_2^2) + s_{58} (h_1 - h_2) - s_{59})}{\sigma \sqrt{1+\lambda_1}}, s_{89} = \frac{(2s_{57} (h_1 - h_2) + s_{58}) s_{35}}{(\sigma \sqrt{1+\lambda_1})^2} \\
 s_{90} &= \frac{2s_{57} s_{36}}{(\sigma \sqrt{1+\lambda_1})^3}, s_{91} = \frac{s_{17}^2 (h_1^5 - h_2^5)}{60} + \frac{s_{32} (h_1^4 - h_2^4)}{12\sigma^2}, s_{92} = \frac{s_{51} (h_1^3 - h_2^3)}{3} + s_{52} (h_1^2 - h_2^2) + s_{53} (h_1 - h_2) \\
 s_{93} &= s_{84} + s_{85} - s_{86} + s_{87}, s_{94} = s_{88} - s_{89} + s_{90} + s_{91} - s_{92}, s_{95} = \left(\frac{s_{35}}{s_2 \sigma \sqrt{1+\lambda_1}} - (h_1 - h_2) \right), \\
 s_{96} &= \frac{(s_4 - s_1) (s_{36} - s_{35})}{\sigma \sqrt{1+\lambda_1} (s_2 s_4 - s_1 s_5)}, s_{97} = \frac{(s_{95} + s_{96})}{\sigma^2}, s_{98} = \frac{Gr (s_{71} + L s_{72}) s_{35}}{\sigma \sqrt{1+\lambda_1}}, s_{99} = \frac{s_{83} Gr (s_{36} + s_{35})}{\sigma \sqrt{1+\lambda_1} (s_2 s_4 + s_1 s_5)} \\
 s_{100} &= s_{98} + s_{99} - Gr (s_{93} + s_{94})
 \end{aligned}$$



(a)



(b)



(c)

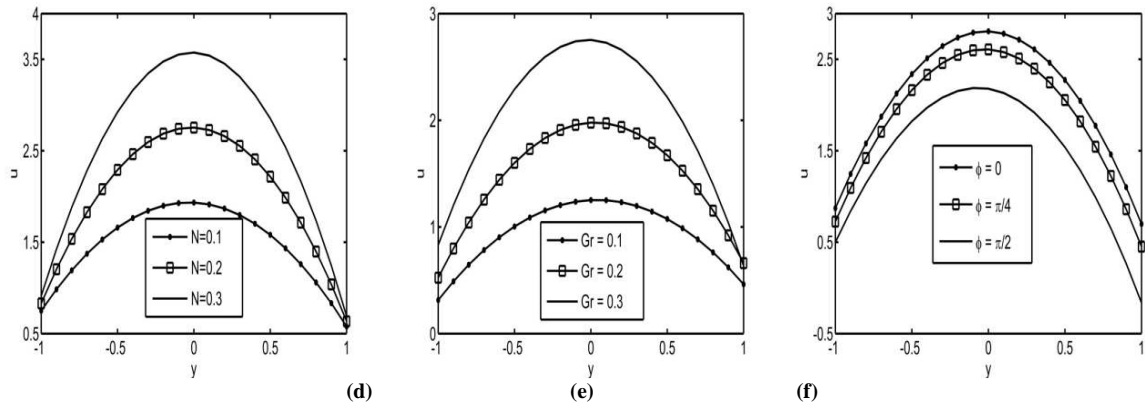


Fig.1 Velocity profiles at $a=0.5, b=0.5, d=1.1, x=0, n=2$ for (a) $\sigma=0.5, N=0.2, \phi=\pi/8, Gr=0.3, L=0.5$ (b) $\lambda_1=0.1, N=0.2, \phi=\pi/8, Gr=0.3, L=0.5$ (c) $\lambda_1=0.1, N=0.2, \phi=\pi/8, Gr=0.3, \sigma=0.5$ (d) $\lambda_1=0.1, L=0.5, \phi=\pi/8, Gr=0.3, \sigma=0.5$ (e) $\lambda_1=0.1, L=0.5, \phi=\pi/8, N=0.2, \sigma=0.5$ (f) $\lambda_1=0.1, L=0.5, Gr=0.3, N=0.2, \sigma=0.5$

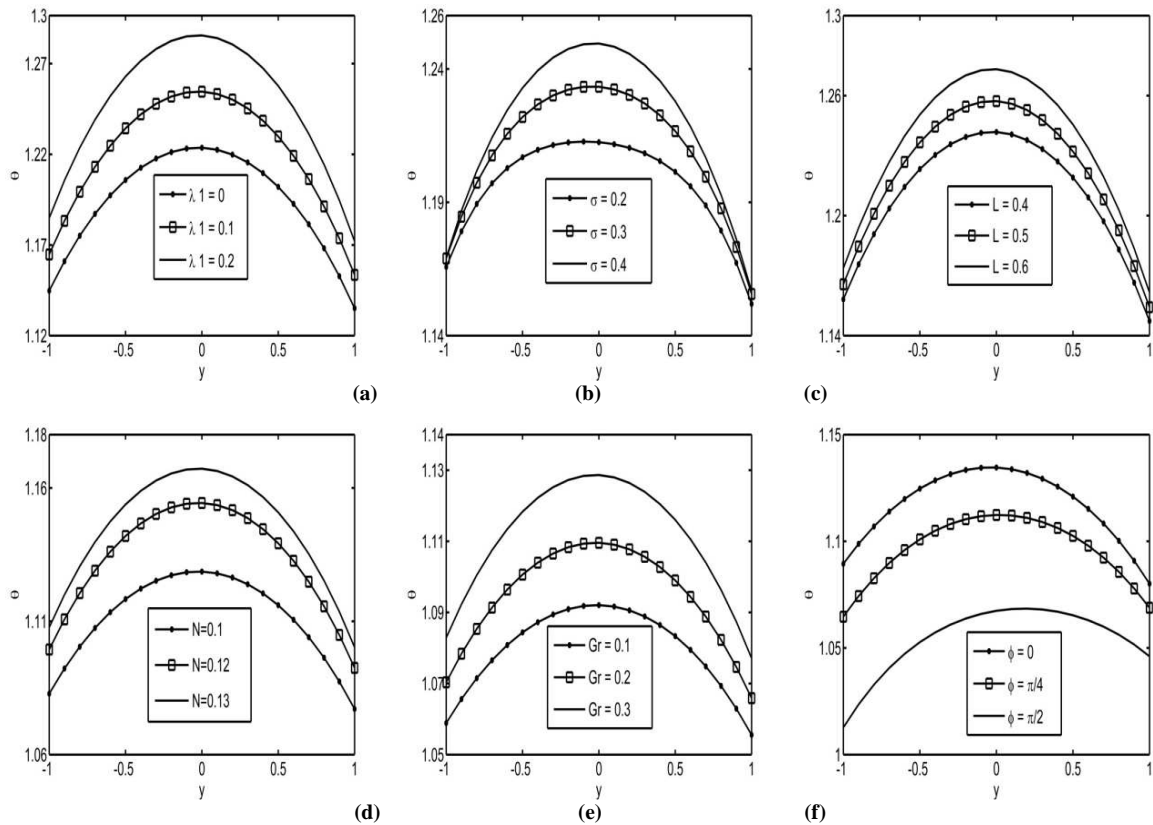


Fig.2 Temperature profiles at $a=0.5, b=0.5, d=1.1, x=0, n=1$ (a) $\sigma=0.5, N=0.2, \phi=\pi/8, Gr=0.3, L=0.5$ (b) $\lambda_1=0.1, N=0.2, \phi=\pi/8, Gr=0.3, L=0.5$ (c) $\lambda_1=0.1, N=0.2, \phi=\pi/8, Gr=0.3, \sigma=0.5$ (d) $\lambda_1=0.1, L=0.5, \phi=\pi/8, Gr=0.3, \sigma=0.5$ (e) $\lambda_1=0.1, L=0.5, \phi=\pi/8, N=0.1, \sigma=0.5$ (f) $\lambda_1=0.1, L=0.5, Gr=0.3, N=0.1, \sigma=0.5$

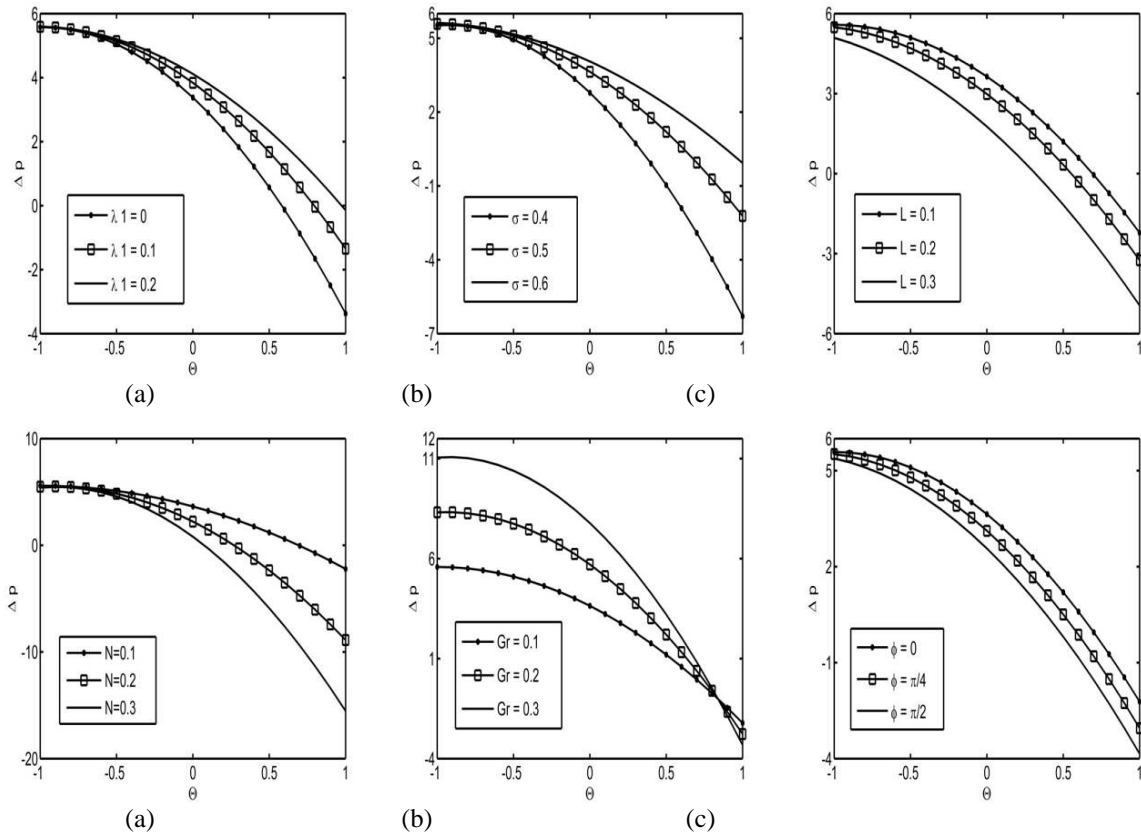


Fig.3 Variation of pressure rise versus flowrate at $a=0.5, b=0.5, d=1, n=0.5$ (a) $\sigma=0.2, N=0.1, \phi=\pi/8, Gr=0.1, L=0.2$ (b) $\lambda_1=0.1, N=0.1, \phi=\pi/8, Gr=0.1, L=0.5$ (c) $\lambda_1=0.1, N=0.1, \phi=\pi/8, Gr=0.1, \sigma=0.2$ (d) $\lambda_1=0.1, L=0.2, \phi=\pi/8, Gr=0.1, \sigma=0.2$ (e) $\lambda_1=0.1, L=0.2, \phi=\pi/8, N=0.1, \sigma=0.2$ (f) $\lambda_1=0.1, L=0.2, Gr=0.1, N=0.1, \sigma=0.2$

REFERENCES

- [1] A.H. Shapiro, M.Y. Jaffrin, and S.L. Weinberg, *J. Fluid Mech.*, **1969**37, 799-825.
- [2] M.J. Manton, *J. Fluid Mech.*, **1975**, 68, 467-476.
- [3] Y.C. Fung and C.S. Yih, *J. Appl. Mech.*, **1968**, 35, 669 – 675.
- [4] M.Y. Jaffrin and A.H. Shapiro, *Ann. Rev. Fluid Mech.*, **1971**, 3, 13-36.
- [5] G. Radhakrishnamacharya, *Rheol. Acta.*, **1982**, 21, 30-35.
- [6] J.B. Shukla and S.P. Gupta, *J. Biomech. Eng.*, **1982**, 104, 182 – 186.
- [7] L.M. Srivastava and V.P. Srivastava, *J. Biomech.*, **1984** 17, 821 – 829.
- [8] S. Takabatake and K. Ayukawa, *J. Fluid Mech.*, **1982**, 122, 439.
- [9] S.L. Weinberg, E.C. Eckstein and A.H. Shapiro, *J. Fluid. Mech.*, **1971**, 49, 461 – 197.
- [10] F. Yin and Y.C. Fung, *J. Fluid Mech.*, **1971**, 47, 93 – 112.
- [11] V.P. Srivastava and M. Saxena, *Rheol. Acta.*, **1995**, 34, 406 – 414.
- [12] S. Sreenadh, P. Lakshminarayana and G. Sucharitha, *Int. J. of Appl. Math. and Mech.*, **2011**, 7(20), 18- 37.
- [13] G. Sucharitha, S. Sreenadh and P. Lakshminarayana, *Int. J. of Eng. Sci. and Tech.*, **2013**, 5(1), 106-113.
- [14] G. Sucharitha, S. Sreenadh and P. Lakshminarayana, *Int. J. of Eng. Research & Technology*, **2012**, 1(10), 1-10.
- [15] S. Srinivas and M. Kothandapani, *Appl. Math. Comput.*, **2009**, 213, 197-208.
- [16] P. Lakshminarayana, S. Sreenadh and G. Sucharitha, *Elixir Appl. Math.*, **2013**, 54, 12413-12419.
- [17] K. Vajravelu, S. Sreenadh and P. Lakshminarayana, *Commun. Non-linear Sci. Numer. Simulat.*, **2011**, 16, 3107-3125.
- [18] R.P. Agarwal, Heat transfer to pulsatile flow of conducting fluid in a porous channel, Ph.d Thesis, Allahabad, **1989**.
- [19] Tang Dalin and M.C. Shen, *Int. J. Eng. Sci.*, **1989**, 27, 809-825.
- [20] G. Radhakrishnamacharya and C.H. Srinivasulu, *C R Mecanique.*, **2007**, 335, 369-373.
- [21] G.S. Beaver and D.D. Joseph, *J. Fac. Educ. Ain Shams Univ. Egypt.*, **1967**, 22, 35-51.

- [22] P.G. Saffman, *Stud. Appl. Math.*, **1971**,50, 93-101.
- [23] K. deVries, E.A. Lyons, G. Ballard, C.S. Levi and D.J. Lindsay, *Am.J.Obstetries Gynecol.***1990**, 62, 679-82.
- [24] J.R. Keener and J. Sneyd, *Mathematical physiology*, Springer, **1998**.
- [25] D.H. Bergel, *Cardiovascular Fluid Dynamic*. Academic Press, London, **1972**.
- [26] A.V. Ramana Kumari and G. Radhakrishnamacharya, Effect of slip on heat transfer to peristaltic transport in the presence of magnetic field with wall effects, **2011**,6, 7.
- [27] M. Arun Kumar, S. Venkataramana, S. Sreenadh and P. Lakshminarayana,*International Journal ofMathematical Archive*,**2012**3, 11.
- [28] T. Hayat, Q. Hussain and N. Ali, *Phys. Lett. A*, **2008**, 387, 3399-3409.
- [29] M. Mishra and A. Ramachandra Rao, *ZAMP*, **2003**, 54, 532-50.
- [30] K. Vajravelu, S. Sreenadh, G. Sucharitha and P. Lakshminarayana,*Int. J. of Biomath.*, **2014**, **7** (6), 1450064 (25 pages).
- [31] S. Sreenadh, P. Lakshminarayana, M. Arun kumar and G. Sucharitha, *International J. of Math. Sci. & Engg. Appls. (IJMSEA)*,**2014**, 8 (V), 27-40.
- [32] P. Lakshminarayana, S. Sreenadh and G. Sucharitha, *Advances in Applied Science Research*, **2012**, 3 (5), 890-2899.